Two-stage Multi-UAV Planning Solution Combining A*, Model Predictive Control, and Artificial Potential Field

Peiyu Yang (5992214), Siqi Pei (5964377), Xiaotong Li (5965373), Ziang Liu (5978866)

Abstract— In this paper, we present a global and local two-stage multi-UAV planning solution that incorporates A*, model predictive control (MPC), and artificial potential field (APF) to realize the path planning of UAV clusters in dynamic environments. This navigation solution can empower multiple UAVs to avoid obstacles and collaborate in complex environments. The video can be accessed at the following link: https://youtu.be/RkOqEFh1KFM

I. INTRODUCTION

With the growing application of UAVs, research on path-planning methods has become a focus of attention. The state of art path planning methods are usually divided into two parts: global and local planning. The typical methods for global planning contain heuristic methods (e.g. A*[1], D*[2]), sampling-based methods (e.g. RRT[3], RRT*[4]), and optimization methods (e.g. PSO[5], ACO[6]). The typical methods for local planning include rolling window algorithms[7], APF[8], and case-based learning methods[9].

Inspired by collaborative multi-UAV missions in sparse woods, we present a two-stage UAV path planning solution. The structure of this planning solution is shown in Fig.1.

The main innovations of this paper are

- A modified RRT* algorithm is proposed to obtain more accurate path planning results for a single UAV system.
- Implementation of a variant of the A* global planning algorithm for equal-level multi-UAV.
- Establishing a local planning and control method for UAVs combining MPC, artificial potential field, and PID methods.

Our solution is designed to address the path planning challenges for multiple UAVs, facilitating conflict resolution and formation control. Compared to the state-of-the-art methods, our method is still deficient in respect of the path of optimality.

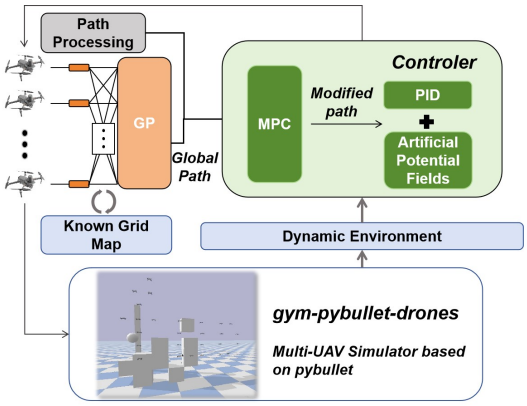

Fig. 1: System structure

II. ROBOT MODEL

We select an X-shaped quadrotor UAV and express the orientation with Euler angles. We only consider the effect of propeller force, torque, and gravity of the UAV.

A. Propeller Model

The thrust force and moment of a propeller can be expressed as

$$\begin{cases} f_i = k_f \omega_i^2 \\ \tau_i = k_\tau \omega_i^2 \end{cases}, \tag{1}$$

where ω_i is the rotate speed of the i-th propeller, k_f, k_τ are the thrust coefficient and reverse torque coefficient.

B. UAV Model

The linear motion equation of the UAV under external force $\vec{F}$ and the angular motion equation of the UAV under external torque $\vec{M}$ are

$$\sum \vec{F} = m \cdot \frac{d\vec{V}}{dt}, \tag{2}$$

$$\sum \vec{M} = \frac{d\vec{L}}{dt}, \tag{3}$$

where m is the mass, $\vec{V}$ is the speed vector, and $\vec{L}$ is the angular momentum vector.

In body frame

$$\vec{F} = \begin{bmatrix} 0 & 0 & U_1 \end{bmatrix}^T - R_{\phi,\theta,\psi} \begin{bmatrix} 0 & 0 & mg \end{bmatrix}^T, \tag{4}$$

$$\vec{M} = \begin{bmatrix} lU_2 & lU_3 & U_4 \end{bmatrix}^T, \tag{5}$$

where

$$\begin{cases} U_1 = (f_1 + f_2 + f_3 + f_4) \\ U_2 = \frac{\sqrt{2}}{2}(-f_1 + f_2 - f_3 + f_4) \\ U_3 = \frac{\sqrt{2}}{2}(-f_1 + f_2 + f_3 - f_4) \\ U_4 = (-\tau_1 - \tau_2 + \tau_3 + \tau_4) \end{cases}, \tag{6}$$

and l is the arm length, ϕ, θ, ψ are the Euler angles, $R_{\phi,\theta,\psi}$ is the rotation matrix under the Euler angles.

Transfer the resultant force in eq.4 to ground frame and apply eq.2, we get

$$\begin{cases} \dot{v}_x = (\cos\phi \sin\theta \cos\psi + \sin\phi \sin\psi) U_1/m \\ \dot{v}_y = (\cos\phi \sin\theta \sin\psi - \sin\phi \cos\psi) U_1/m \\ \dot{v}_z = \cos\phi \cos\theta \cdot U_1/m - g \end{cases}, \tag{7}$$

where v_x, v_y, v_z are the velocity components of the UAV.

Transfer the resultant torque in eq.5 to ground frame and apply eq.3, we get

$$\begin{cases} M_x = \dot{\omega}_x \cdot I_x + \omega_y \cdot \omega_z (I_z - I_y) \\ M_y = \dot{\omega}_y \cdot I_y + \omega_x \cdot \omega_z (I_x - I_z) \\ M_z = \dot{\omega}_z \cdot I_z + \omega_x \cdot \omega_y (I_y - I_x) \end{cases}, \tag{8}$$

where ω_x, ω_y, ω_z are the angular velocity components of the UAV, I_x, I_y, I_z are the momentum of inertia of the UAV in three axes.

Apply small angle approximation

$$\begin{bmatrix} \omega_x & \omega_y & \omega_z \end{bmatrix}^T = \begin{bmatrix} \dot{\phi} & \dot{\theta} & \dot{\psi} \end{bmatrix}^T, \tag{9}$$

and combine eq.7 and eq.8, we can get the math model of the quadrotor UAV[10]:

$$\begin{cases} \ddot{x} = (\cos\phi \sin\theta \cos\psi + \sin\phi \sin\psi) U_1/m \\ \ddot{y} = (\cos\phi \sin\theta \sin\psi - \sin\phi \cos\psi) U_1/m \\ \ddot{z} = \cos\phi \cos\theta \cdot U_1/m - g \\ \ddot{\phi} = \left[l \cdot U_2 + \dot{\theta}\dot{\psi} (I_y - I_z) \right] / I_x \\ \ddot{\theta} = \left[l \cdot U_3 + \dot{\phi}\dot{\psi} (I_z - I_x) \right] / I_y \\ \ddot{\psi} = \left[U_4 + \dot{\phi}\dot{\theta} (I_x - I_y) \right] / I_z \end{cases} \tag{10}$$

C. Workspace and Configuration Space

In our path planning problem, we only focus on the position of the UAVs and don't care about their orientation, so we used the differential flatness model when controlling the UAVs. In this way, the workspace can be simplified to $\mathbb{R}^3$ (3D position), and the configuration space can be simplified to $\mathbb{R}^3 \times \mathbb{S}^1$ (3D position and yaw).

From eq.10, we know that the height and yaw control are independent, but the horizontal control is coupled with pitch and roll control, therefore we can control the UAV with 4 command variables: x, y, z, ψ, and we can always set $\psi = 0$ because we only care about the position.

PID controller is selected for position and orientation control.

III. MOTION PLANNING

In this section, we will introduce the planning methods, global planning, and local planning respectively. Due to the page limitation, the pseudocode of the algorithms covered in this section will be given in the presentation.

A. Global Planning

1) Modified RRT*: In the global planning section, we have modified the traditional RRT* algorithm to make the plan. Specifically, the RRT* algorithm we used before selects the parent node only one time after inserting the new node, so we add a step after choosing the parent node for a new node, which is we will refresh all the parent nodes in the parent range, to find if the new inserting node could provide

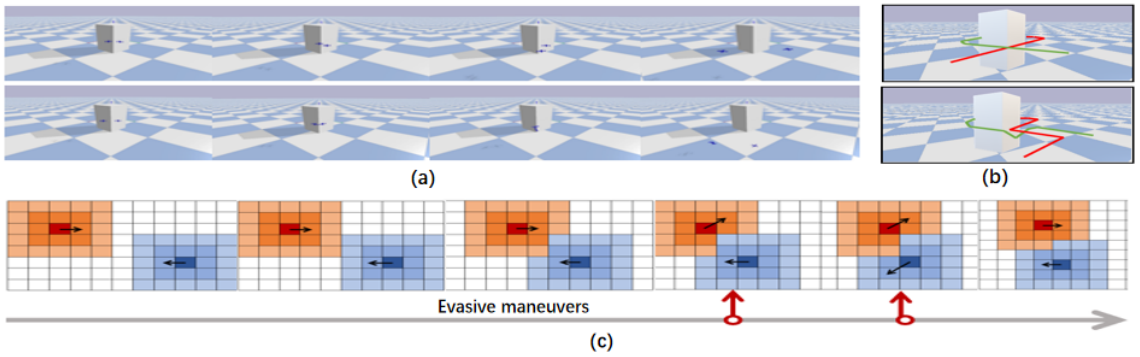

Fig. 2: Modified A* algorithm. (a) The simulation process. (b) The generated path. (c) The map updating process.

them a shorter way to the starting node, as Fig.6 shows.

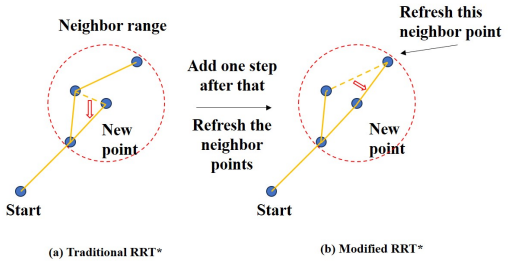

Fig. 3: Modified the traditional RRT* to make global planning. (a) Traditional RRT*. (b) M-RRT*

2) Equal-level multi-core A* algorithm: We present an A* algorithm for the global planning of Equal-level multi-UAV tasks. This algorithm considers all UAVs in the obstacle space and updates the global map in each planning loop to enable individual UAVs to obtain heuristically generated trajectories without colliding with other UAVs. The global map update and UAV evasion are shown in Fig.2(c)

B. Local Planning

1) MPC: In the local planning section, we first use MPC control to avoid moving obstacles and decrease the energy cost during the process, the equation of the MPC is shown as follows:

$$\begin{aligned} \min_{\mathbf{u}} \quad & \sum_{k=0}^{N-1} \|x_k - r_k\|_Q^2 + \|u_k\|_R^2 \\ \text{s.t.} \quad & x_{k+1} = Ax_k + Bu_k, \\ & C_t x_k \geq y_t, \\ & u_{\min} \leq u_k \leq u_{\max}, \end{aligned} \tag{11}$$

where N is the prediction horizon, r_k is the reference trajectory, and Q and R are positive definite weighting matrices.

Considering that the solver could only handle linear constraints, so we have to transfer the moving object to a linear constraint. In detail, we make a new plane between the UAV and the moving obstacle which is at a given meter from the moving obstacle as Fig.4 shows, and it could certificate that the UAV will not hit on the moving obstacle.

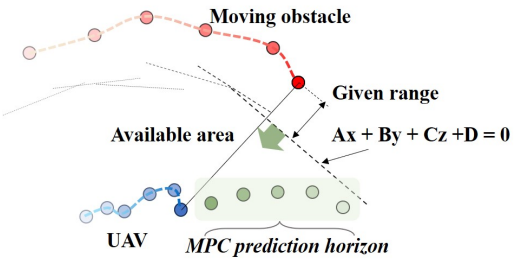

Fig. 4: Transfer the moving object to a linear constraint.

2) Artificial Potential Field: We also implemented an artificial potential field to avoid local obstacles. When the drones go close enough to obstacles (including other drones), they will be repelled away by a force. We choose the closest point on each obstacle to compute the repel field to simplify the model, as shown in Fig.5.

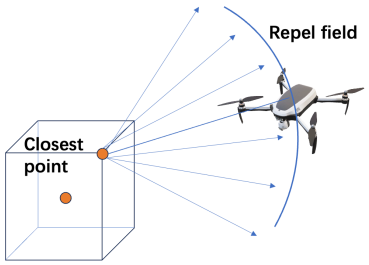

Fig. 5: Choose the closest point on the obstacle to compute the repel field

For drone flocks, we added an attraction field between each drone and its closest neighbor. We also add an attraction field between each drone and its goal to prevent it from being misguided away, because of other convoluted potential fields, from the path given by the global planner to somewhere else. The equation below explains the principle of our artificial potential field, in which V_{dir} denotes the direction vector and I denotes intensity.

$$\begin{cases} V_{\text{dir}} = P_{\text{self}} - P_{\text{oth/obs}} & \text{(Repel field)} \\ V_{\text{dir}} = P_{\text{oth/obs}} - P_{\text{self}} & \text{(Attraction field)} \end{cases} \tag{12}$$

$$\begin{cases} U_{\text{rep}} = I \times V_{\text{dir}} \times (1/\text{dis}^2 - 1/\text{ran}^2) \\ U_{\text{att}} = I \times V_{\text{dir}} \times \text{dis}^2 \end{cases} \tag{13}$$

IV. RESULTS

A. Results of Subsystem Simulation

1) Comparative Experiments on Global Planning Methods: To determine the specific global planning method used, we designed the simulation experiment used to compare the RRT*, Modified RRT*, and A* algorithms. The results of this experiment are shown below:

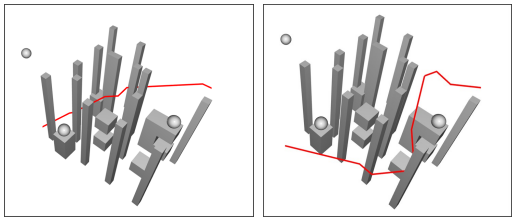

Fig. 6: Path planning for single UAV with modified A* and RRT*

TABLE I: Data for modified A* and RRT*

Method	Time cost (s)	Path length (m)	Energy consumption (Norm)
A*	9.13	7.27	0.9070
RRT*	37.72	13.93	1.0000
M-RRT*	36.27	7.50	0.9515

where all RRT methods used 500 iterations as the hyperparameter.

The experiment results show that the modified RRT* method obtains significantly better path lengths than the RRT* method in approximate computation time, while the A* method obtains the best path lengths in the shortest computation time. Considering that the A* algorithm can solve the multi-UAV path conflict problem by applying an update to the global map, while the RRT*-based methods are difficult to extend to multi-UAV scenarios, we chose to use the A* method as the global path planning method in the subsequent experiments.

An experiment has been designed for the modified A* method, where the start and target points of two UAVs are designed to produce path-conflicting configurations.

In this experiment, the trajectories generated by the traditional A* algorithm resulted in

UAVs colliding with each other at the conflict points, while the modified A* method resulted in the separation of the generated trajectories and successfully solved the UAV collision problem as shown in Fig.2(a).

2) Local planning experiment: The experimental results show that the MPC caused the UAVs to avoid approaching a moving obstacle, and the artificial potential field caused the UAVs to maintain a safe distance when the distance between the UAVs was less than the range of the artificial potential field.

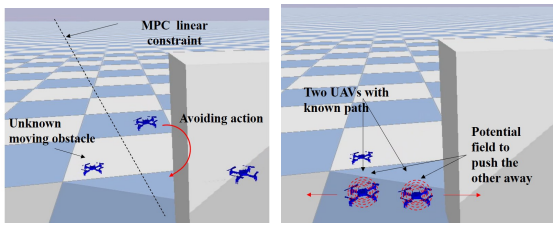

Fig. 7: Avoiding moving obstacle with MPC and known UAV with potential field

B. Overall Experiment

In the overall experiment, we designed a formation of 27 UAVs to transform from an initial 18-shaped pattern to a TUD badge-shaped pattern after passing through a space where obstacles are present. During the experiment, the 27 UAVs completed the planning tasks for each subsystem while no UAVs collided throughout.

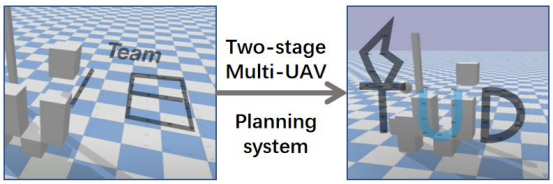

Fig. 8: Overall experiment for the whole system.

V. DISCUSSION

A. Methods Discussions

RRT*, Modified RRT* and A* are the alternatives we are planning for globally. This problem has a time and results trad-off. As illustrated in Fig.9, it is evident that the A* algorithm results in points closer to the origin, indicating superior algorithmic performance.

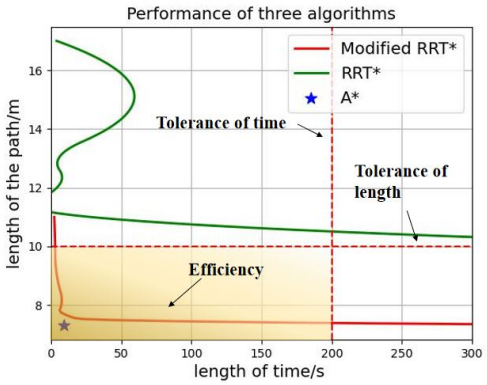

Fig. 9: Analysis of global planning methods. The data in the figure are obtained from experimental data with interpolation analysis.

The Two-Stage Multi-UAV Planning Solution we provide has advantages in the perspective of multi-UAV formation and UAV collision avoidance in sparse forests, but due to its use of more planning methods, it can lead to still incorrect interference between UAVs in more complex and narrower scenarios, which is fatal for some special cases. In global planning, limited by the discrete maps used by the A* algorithm, the corners of the planned paths are not continuous, so the resulting maps are sub-optimal solutions. Also due to the use of MPC and artificial potential field methods, we need to carefully adjust the hyperparameters to make them match the real-time and task requirements

B. Future Work

In the future, we will focus on three aspects of this research based on weaknesses

- Solving angle problems in uniformly discrete maps[11] using interpolate methods.
- Extending the MPC method to nonlinear models to further increase accuracy.
- Using the state classification design AFP applicable to narrow environment.

References

[1] P. E. Hart, N. J. Nilsson, and B. Raphael, "A formal basis for the heuristic determination of minimum cost paths," IEEE transactions on Systems Science and Cybernetics, vol. 4, no. 2, pp. 100–107, 1968.

[2] D. Ferguson and A. Stentz, "Using interpolation to improve path planning: The field d* algorithm," Journal of Field Robotics, vol. 23, no. 2, pp. 79–101, 2006.

[3] Y. Shang, F. Liu, P. Qin, Z. Guo, and Z. Li, "Research on path planning of autonomous vehicle based on rrt algorithm of q-learning and obstacle distribution," Engineering Computations, vol. 40, no. 5, pp. 1266–1286, 2023.

[4] S. Yu, J. Chen, G. Liu, X. Tong, and Y. Sun, "Sof-rrt*: An improved path planning algorithm using spatial offset sampling," Engineering Applications of Artificial Intelligence, vol. 126, p. 106875, 2023.

[5] S. Lin, A. Liu, J. Wang, and X. Kong, "An intelligence-based hybrid pso-sa for mobile robot path planning in warehouse," Journal of Computational Science, vol. 67, p. 101938, 2023.

[6] Z. A. Ali, H. Zhangang, and D. Zhengru, "Path planning of multiple uavs using mmaco and de algorithm in dynamic environment," Measurement and Control, vol. 56, no. 3-4, pp. 459–469, 2023.

[7] C.-C. Chou, F.-L. Lian, and C.-C. Wang, "Characterizing indoor environment for robot navigation using velocity space approach with region analysis and look-ahead verification," IEEE Transactions on Instrumentation and Measurement, vol. 60, no. 2, pp. 442–451, 2010.

[8] H. M. Jayaweera and S. Hanoun, "A dynamic artificial potential field (d-apf) uav path planning technique for following ground moving targets," IEEE access, vol. 8, pp. 192 760–192 776, 2020.

[9] M. F. Abdelwahed, A. E. Mohamed, and M. A. Saleh, "Solving the motion planning problem using learning experience through case-based reasoning and machine learning algorithms," Ain Shams Engineering Journal, vol. 11, no. 1, pp. 133–142, 2020.

[10] E. Altug, J. Ostrowski, and R. Mahony, "Control of a quadrotor helicopter using visual feedback," in Proceedings 2002 IEEE International Conference on Robotics and Automation (Cat. No.02CH37292), vol. 1, 2002, pp. 72–77 vol.1.

[11] F. Duchoň, A. Babinec, M. Kajan, P. Beňo, M. Florek, T. Fico, and L. Jurišica, "Path planning with modified a star algorithm for a mobile robot," Procedia engineering, vol. 96, pp. 59–69, 2014.